

See discussions, stats, and author profiles for this publication at: <https://www.researchgate.net/publication/250134270>

The Archaeometallurgy of War Kabud, Western Iran

Article in *Iranica Antiqua* · January 2006

DOI: 10.2143/IA.41.0.2004759

CITATIONS

12

READS

162

6 authors, including:



Vincent C. Pigott

University of Pennsylvania

45 PUBLICATIONS 654 CITATIONS

[SEE PROFILE](#)



Ernie Haerinck

Ghent University

101 PUBLICATIONS 229 CITATIONS

[SEE PROFILE](#)



B. Overlaet

Royal Museums of Art and History, Brussels

66 PUBLICATIONS 143 CITATIONS

[SEE PROFILE](#)

Some of the authors of this publication are also working on these related projects:



Saruq al-Hadid Archaeological Research Project [View project](#)



Royal Museums of Art and History Brussels [View project](#)

THE ARCHAEOMETALLURGY OF WAR KABUD, WESTERN IRAN

BY

S.J. FLEMING*, V.C. PIGOTT**, C.P. SWANN*, S.K. NASH*,
E. HAERINCK*** and B. OVERLAET***

(* MASCA, University of Pennsylvania Museum, Philadelphia, PA., USA;

** Institute of Archaeology, University College London, UK &

*** Ghent University, Belgium)

The Belgian Archaeological Mission in Iran (BAMI) started its research in the Pusht-i Kuh of Luristan in the autumn of 1965. The BAMI was a joined effort of Ghent University and the Royal Museums of Art and History, Brussels (KMKG-MRAH). The expeditions which were directed until 1979 by the late Louis Vanden Berghe, targeted mainly graveyards from the Chalcolithic era, the Bronze Age and the Iron Age (Haerinck & Overlaet 1996, p. 1-6; 2004b). War Kabud is the first and the largest of the Iron Age III cemeteries (ca. 800/750 to 600 BCE) that were excavated.

The graveyard of War Kabud is situated about 25 km northwest of Ilam, on a small plateau between mountains and the Lashkan, a small tributary of the Chavar river (fig. 1). Local villagers had looted a large part of the graveyard and it was estimated that about 1.000 tombs had already been robbed before the expedition arrived at the site (fig. 2). During two consecutive years, 1965 and 1966, the BAMI expedition worked at War Kabud. Each year, they excavated a large untouched area and some tombs in the plundered areas that had been missed by the looters.

A total of 203 tombs were registered. 153 of these were located in the two undisturbed areas and were given the prefix "A" (tombs A1 to A150 and tombs A81bis, A119bis and A131bis), and 50 were located between the plundered tombs. These 50 were given the prefix "B" (B151 to B200).

The burial goods in each tomb were also given a consecutive number. The inventory numbers of the finds thus provide a reference to the tombs they were found in. The macehead with the inventory number WK.B191-3,

which is discussed *infra*, is for example, the third registered object (–3) from tomb B191 (B indicates that it was located between the plundered tombs) at War Kabud (WK). It is an easy reference system that is used throughout the final report on the War Kabud excavations (Haerinck & Overlaet 2004a).

A selection of the finds from War Kabud was donated to the Royal Museums of Art and History, Brussels. The remainder of the finds was deposited in the Iran National Museum in Teheran. 48 of the objects in Brussels were selected and sent to MASCA (Museum Applied Science Center, University of Pennsylvania) for technical analysis (figs. 3-6).

The tombs at War Kabud are all individual. Several types of tombs were encountered. There were simple “pit tombs”, sometimes fully or partly covered with stone boulders or slabs, and more complex “cist tombs” which had at least one wall constructed with stone boulders or slabs. The most elaborate ones had four stone walls and a stone cover. Some of the analysed objects come from what was called a “horse burial” (tomb A150). It consisted of a horse bit, phalera, buttons, large rings, bells and an iron stake which were found underneath some stones. It remains uncertain, however, whether it was a true horse burial as the presence of a horse skeleton could not be confirmed (Haerinck & Overlaet 2004a, p. 54, fig. 19, pl. 57, 128).

Burial goods were found in 177 tombs, usually only three to seven objects were present. Pottery was the vast majority (46%). Iron was mostly used for utilitarian objects (arrowheads, axes, swords...) while bronze was mainly confined to jewellery (rings, anklets, bracelets...), luxury items (goblets, bowls and vases), specific groups of armament (maceheads and a decorated axe-adze) or decorative mountings (sword grips, quiver plaque). Silver and gold were very rare and were only used for small jewellery such as earrings or beads. The War Kabud metal assemblage is thus conform to the general picture we have of the Iron Age III metalwork in the Pusht-i Kuh, known from sites such as Chamahzi Mumah (Haerinck & Overlaet 1998), Djub-i Gauhar and Gul Khanan Murdah (Haerinck & Overlaet 1999). The Iron Age III apparently represents a relative prosperous period with an increased population density in Pusht-i Kuh, compared to the preceding Early Iron Age during which metal burial goods are less common and imports from Mesopotamia are rare (Overlaet 2003; 2005).

The forty-eight selected bronzes from War Kabud were analysed for alloy and composition using proton-induced x-ray emission (PIXE) spectrometry (see Fleming and Swann 1993; Swann et al. 1992). The microstructures of eight of these were studied using standard metallographic microscopy (see Scott 1991) to determine the manner and extent to which their metal had been manipulated after casting. With the exception of the unique quiver plaque from tomb A10 (Haerinck & Overlaet 2004a, p. 52-53, fig. 18, pl. 129) and the decorated axe-adze from tomb B188 (Haerinck & Overlaet 2004a, p. 48-49, fig. 16, pl. 66, 124), every type of bronze from the graveyard is represented in this analytical program to some extent — notably, three of the eight maceheads and one of the two bronze fibulae (see fig. 3-6) — so we believe that the technological conclusions we draw are reasonably representative of the entire War Kabud bronze corpus.

The PIXE data are presented in detail in Table 1 and summarized in Table 2. Among the nineteen jewellery items, the tin content varies from 3.4% to 12.7%, with a mean of 7.6% ($\pm 0.7\%$, one standard error).

Table 1. Composition of copper-base artifacts from various burials at War Kabud*

Site reference	Object	Cu	As	Sn	Fe	Pb	Ni	Ag	Sb
<i>jewellery</i>									
WK.A6-6	anklet	90.8	0.20	7.8	0.11	0.028	0.117	0.030	0.063
WK.B171-4	anklet	90.5	0.53	6.1	0.35	1.2	0.185	0.121	0.43
WK.A102-5	anklet	86.1	0.39	11.3	0.20	0.91	0.114	0.115	0.076
WK.A1-4	bracelet	86.0	0.14	12.4	0.22	0.10	0.187	≤ 0.029	≤ 0.053
WK.B185-3	fibula	90.5	0.16	7.9	0.04	0.16	0.268	0.039	≤ 0.038
WK.A76-5	finger ring	87.6	0.56	9.8	0.13	0.80	0.108	0.098	0.16
WK.B200-1	finger ring	93.7	1.20	3.4	0.42	0.20	0.165	0.107	0.21
WK.A92-4	finger ring	92.6	0.05	4.3	0.25	0.62	0.084	0.126	≤ 0.022
WK.A94-5	finger ring	90.7	1.33	6.7	0.37	0.053	0.092	≤ 0.021	≤ 0.041
WK.B155-2	pin	88.4	0.25	10.1	0.12	0.26	0.106	0.067	0.11
WK.B186-4	pin	94.9	0.66	4.1	0.21	0.061	0.104	≤ 0.020	≤ 0.025
WK.A43-6	pin	90.7	0.28	7.7	0.16	0.16	0.096	0.038	0.096
WK.A22-3	pin	87.9	0.33	9.0	0.19	0.61	0.105	0.094	0.18
WK.A140-5	pin	88.2	0.16	10.3	0.21	0.10	0.088	≤ 0.016	≤ 0.028
WK.A68-6	ring	85.4	0.13	12.7	0.19	0.026	0.088	0.034	≤ 0.058
WK.A150-8	ring	91.4	0.39	6.4	0.11	0.25	0.120	0.12	0.14
WK.A56-4	ring	92.2	0.58	4.0	0.49	0.87	0.096	0.107	0.29
WK.A49-5	ring	94.6	0.300	3.6	0.18	0.087	0.170	≤ 0.011	0.082
WK.B199-3	ring	91.4	0.24	6.0	0.14	1.3	0.123	0.083	0.080

Site reference	Object	Cu	As	Sn	Fe	Pb	Ni	Ag	Sb
<i>vessels</i>									
WK.B196-5	vessel	94.4	0.51	3.1	0.55	0.26	0.082	0.135	0.22
WK.B157-3	vessel	89.0	0.13	9.7	0.10	0.23	0.100	0.057	0.065
WK.B167-2	vessel	94.3	0.41	2.6	0.37	1.08	0.091	0.129	0.33
WK.B194-4	vessel	88.2	≤ 0.01	10.9	0.10	0.21	0.077	0.027	≤ 0.027
WK.B183-6	vessel	89.2	0.25	8.7	0.21	0.49	0.088	0.113	0.17
WK.B192-4	vessel	90.9	0.25	7.4	0.13	0.26	0.080	0.123	0.17
WK.B169-5	vessel	91.8	1.61	5.3	0.15	0.44	0.102	0.074	≤ 0.053
WK.B198-6	vessel	86.2	0.31	12.0	0.21	0.26	0.193	0.034	0.15
WK.A22-4	vessel	90.8	0.28	8.0	0.10	0.17	0.075	≤ 0.014	≤ 0.026
WK.A25-5	vessel	84.8	0.30	13.7	0.11	0.14	0.153	0.039	≤ 0.051
WK.A133-7	vessel	89.0	0.20	9.0	0.07	0.54	0.103	0.103	0.27
WK.A103-6	vessel	86.7	0.10	11.0	0.09	0.91	0.143	0.053	≤ 0.027
WK.A107-5	vessel	87.5	0.31	10.7	0.12	0.37	0.110	0.072	0.095
WK.A123-6	vessel	80.4	0.06	18.2	0.15	0.11	0.066	0.051	≤ 0.041
WK.A46-5	vessel	87.9	0.33	9.5	0.10	0.90	0.111	0.107	0.14
WK.A77-6	vessel	84.0	0.21	8.6	0.15	1.2	0.086	0.099	0.15
WK.B152-6	vessel	88.9	0.14	9.5	0.17	0.29	0.167	0.103	≤ 0.053
WK.B154-5	vessel	90.1	0.25	8.3	0.11	0.030	0.356	0.024	≤ 0.054
WK.A68-7	vessel	89.9	0.06	9.1	0.16	0.021	0.081	0.048	≤ 0.025
WK.A54-7	vessel	88.0	0.21	10.3	0.08	0.70	0.077	0.031	≤ 0.027
WK.A59-8	vessel	86.9	0.03	12.1	0.10	0.022	0.076	0.033	≤ 0.028
WK.A10-6	vessel	89.1	0.06	9.6	0.10	0.16	0.089	0.033	≤ 0.031
<i>others</i>									
WK.B191-3	macehead	91.4	0.35	6.7	0.22	0.26	0.197	0.067	0.094
WK.A5-6	macehead	88.7	0.25	9.9	0.11	0.083	0.116	0.040	0.063
WK.B181-4	macehead	88.3	0.62	8.5	0.16	1.1	0.092	0.124	0.31
WK.A150-5	button**	88.5	0.71	6.9	0.15	2.0	0.110	0.141	0.48
WK.A150-9	button**	88.4	≤ 0.01	10.0	0.29	0.13	0.096	0.121	≤ 0.028
WK.A150-12	bell	86.9	1.45	3.6	0.075	5.1	0.095	0.228	≤ 1.11

* The sulphur content was also measured, but it has been found to vary by a factor of two or more, depending upon where on the artifact the PIXE analysis was carried out. Such variability is not unique to this War Kabud study, however, it has been found in every MASCA project on Near Eastern copper-base artifacts.

** The many buttons found in tomb A150 are thought to have been part of a horse harness and so are not characterized as “jewellery” in this project (see Haerinck & Overlaet 2004b, p. 57).

Table 2. Summary of compositional data for jewellery and vessels from War Kabud

	mean	standard error
<i>Jewellery (n = 19)</i>		
copper (Cu)	90.1%	± 0.6%
arsenic (As)	0.41%	± 0.08%
tin (Sn)	7.6%	± 0.7%
iron (Fe)	0.22%	± 0.03%
lead (Pb)	0.41%	± 0.10%
silver (Ag)	0.067%	± 0.010%
nickel (Ni)	0.13%	± 0.01%
antimony (Sb)	0.11%	± 0.02%
<i>Vessels (n = 23)</i>		
copper (Cu)	88.5%	± 0.6%
arsenic (As)	0.26%	± 0.07%
tin (Sn)	9.5%	± 0.7%
iron (Fe)	0.16%	± 0.02%
lead (Pb)	0.38%	± 0.07%
silver (Ag)	0.067%	± 0.008%
nickel (Ni)	0.11%	± 0.01%
antimony (Sb)	0.10%	± 0.02%

Among the twenty-three vessels (cups and bowls with varying degrees of decoration on them) the tin content varies from 2.6% to 18.2%, with a mean of 9.5% ($\pm 0.7\%$, one standard error).

What is immediately striking is that there is no apparent correspondence between the amount of tin being added to produce the bronze stock and the function of the items fashioned from that stock. The patterns of variability of tin contents among jewellery items and domestic vessels are essentially the same and quite variable (table 1, fig. 7). Among the jewellery and perhaps among the vessels as well, since they now are interpreted as somewhat prestigious grave goods, we might have expected tin contents consistently in excess of 12%, so that the reddish-orange of copper was altered to a golden-yellow (Chase 1983).

The three maceheads, with their tin contents of 6.7%, 8.5%, and 8.9%, will have cast well, since tin at those levels will promote fluidity in an alloy's melt and decreases the absorption of gas that might create damaging porosity during the casting process.

The two buttons from tomb A150 (figs. 3 and 5), with tin contents of 6.9% and 10.0%, will have had a quite attractive orange-golden color;

whether with intent or not, we cannot say. The bell from that same tomb is also interesting (figs. 3 and 5), since it contains so much lead (5.2%). The bell's tin content of only 3.6% will have made its alloy melt only moderately fluid, but the lead will have increased the fluidity appreciably, and made this quite complex little object that much easier to finish later on.

Microstructural data obtained from sections taken from eleven of the artifacts in this project are presented in figures 8–18 (the various technical terms such as “etchant” that are used in the captions of these figures are defined in and illustrated in the MASCA website (<http://masca.museum.upenn.edu/archaeometallurgy.html>)). These data form the basis of the commentary on the technology of Luristan metal production and artifact manufacture that follows.

With the advent of the Iron Age in Luristan, metalworkers who presumably resided there, had available to them a full repertoire of techniques for the casting and shaping of tin-bronze, the period's copper-base alloy of choice. Despite the fact that by the Iron III period production of the canonical “Luristan Bronzes” was clearly on the wane since none were excavated at War Kabud, the breadth of expertise of Iron Age metalworkers is well represented among the War Kabud artifacts analysed here.

Luristan metalworkers clearly were capable of shaping tin-bronze to suit their task-performing requirements as well as their aesthetic, symbolic and cultural norms. Their repertoire of techniques and their *chaîne opératoire* of production were simple but effective. They comprised for the most part the melting of ingots of bronze, imported it has been argued from Mesopotamia (Haerinck and Overlaet 2000; Fleming *et al.* 2005). Luristan is not known for having copper ore deposits and regional archaeology has yet to yield any artifactual evidence of copper smelting and casting (e.g., furnaces, crucibles and/or molds). Molten bronze was cast into basic shapes, often perhaps simple blanks that were worked to shape. In order to achieve the final desired shape of an item in bronze, this step was followed by alternating sequences of cold-working (which hardens bronze) and annealing (which softens bronze and permits its further working). These sequences often obliterate microstructural evidence of the initial casting of the metal, thus making it difficult for us to recreate the full production sequence.

In addition, just as we know virtually nothing of the workshops (presumably located in Luristan) where such work was carried out, we also know nothing of the tools used to work the tin-bronze to shape. It is often

the case that, during this final stage of working some sort of blade, the metalworker did not always leave it in its optimum state, i.e., even in the Iron Age, cutting edges are not always work-hardened and sometimes are even left annealed. Meanwhile, decorative items often can have surfaces that were necessarily hardened by cold-working to achieve their final shape.

The discussion of compositional data earlier in this article raised the point that Luristan metalworkers did not control tin content in relation to artifact type. What this technological randomness suggests is a generalized concern with achieving a desired final shape rather than meeting set or pre-set, standardized mechanical performance parameters for artifacts. Thus, all things considered, to describe those who created the various bronzes entombed at War Kabud and other Luristan necropoli, the term “artisan” or “craftworker” seems more apropos than say “metalworker” or “metalsmith.”

The bell (figs. 3 and 5: WK.A150-12) deserves special note here. It has a microstructure that indicates it was cast to shape but not subsequently worked. This artifact stands out in the War Kabud program by virtue of its unusually complex alloy composition (Cu, 86.9%; Sn, 3.6%; As, 1.4%; Pb, 5.1% and Sb, 1.1%). One is tempted to label the presence of lead as an additive that was designed to enhance fluidity of the metal, something that would have facilitated the bell’s casting. If, however, Luristan craftworkers were working with imported ingots, they will have had little opportunity to control the composition of their final products, except by long experience in judging the nature of their stock by its color. It is more likely that the metal used to cast this bell was smelted from a complex copper sulfide ore that already contained arsenic and antimony. Such ores, the so-called *fahlerz* or grey coppers (e.g., ores in the tennantite to tetrahedrite series, depending on where they occur in ore bodies), commonly intergrow with lead-rich minerals (Thilo Rehren: personal communication).

Four of the analysed War Kabud bronzes (finger rings WK.B200-1 and WK.A94-5, vessel WK.B169-5, bell WK.A150-12) have As-contents of more than 1%, which suggests that complex copper ore bodies containing arsenic were still being exploited even as late as the Iron Age, but arsenic-rich ore bodies are rather rare on the Iranian Plateau. These data therefore may lend further credence to the suggestion made earlier, that the copper-base metal being used in Luristan bronze manufacture was coming from elsewhere, most likely via Mesopotamia.

Bibliography

- CHASE, W.F., 1983, Bronze Casting: A Technical History. *G. Kuwayama (ed.): The Great Bronze Age of China*. Seattle, 1983, p. 100-123.
- FLEMING, S.J. & SWANN, C.P., 1993, Recent Applications of PIXE Spectrometry in Archaeology Part I: Observations on the Early Development of Copper Metallurgy in the Old World. *Nuclear Instruments and Methods in Physics Research B75*, 1993, p. 440-444.
- FLEMING, S.J., PIGOTT, V.C., SWANN, C.P. & NASH, S.K., 2005, Bronze in Luristan: Preliminary Analytical Evidence from Copper/Bronze Artifacts Excavated by the Belgian Expedition in Iran. *Iranica Antiqua XL (Proceedings of the International Conference "The Iron Age in the Iranian World" at Ghent, 17-20 November 2003)*, 2005, p. 35-64.
- HAERINCK, E. & OVERLAET, B., 1996, *The Chalcolithic Period, Parchinah and Hakalan*. (Luristan Excavation Documents I), Brussels, 1996.
- , 1998, *Chamahzi Mumah. An Iron Age III Graveyard*. (Luristan Excavation Documents Vol. II), Acta Iranica 33, troisième série, vol. XIX, Leuven, 1998.
- , 1999, *Djub-i Gauhar and Gul Khanan Murdah. Iron Age III graveyards in the Aivan plain*. (Luristan Excavation Documents Vol. III), Acta Iranica 36, troisième série, vol. XXII, Leuven, 1999.
- , 2000, The Chalcolithic and Early Bronze Age in Pusht-i Kuh, Luristan (West-Iran): Chronology and Mesopotamian Contacts. *Akkadica* 123, 2000, p. 163–181.
- , 2004a, *The Iron Age III graveyard at War Kabud, Pusht-i Kuh, Luristan*. (Luristan Excavation Documents V), Acta Iranica 42, troisième série, vol. XXVII, Leuven, 2004.
- , 2004b, The Chronology of the Pusht-i Kuh, Luristan. Results of the Belgian Archaeological Mission in Iran. *From Handaxe to Khan, essays presented to Peder Mortensen on the occasion of his 70th birthday* (Kj. Von Folsach, H. Thrane & I. Thuesen, eds.), Aarhus, 2004, p. 119-135.
- OVERLAET, B., 2003, *The Early Iron Age in Pusht-i Kuh, Luristan*. (Luristan Excavation Documents IV), Acta Iranica 40, troisième série, vol. XXVI, Leuven, 2003.
- , 2005, The Chronology of the Iron Age in the Pusht-i Kuh, Luristan. *Iranica Antiqua XL (The Iron Age in the Iranian World, Proceedings of the International Congress, Ghent 17-20 November 2003)*, 2005, p. 1-33.
- SCOTT, D.A., 1991, *Metallography and Microstructure of Ancient and Historic Metals*. The J. Paul Getty Museum, Malibu CA, 1991, p. 5-29.
- SWANN, C.P., FLEMING, S.J. & JAKSIC, M., 1992, Recent Applications of PIXE Spectrometry in Archaeology I: Characterization of Bronzes with Special Consideration of the Influence of Corrosion Processes on Data Reliability. *Nuclear Instruments and Methods: Physics Research B49*, 1992, p. 499-504.

Table 3. Reference list of analysed objects from War Kabud

Inv. nr.	object	illustration	Excavation report
WK.A6-6	anklet		Haerinck & Overlaet 2004a, p. 64-65, fig. 23, pl. 7
WK.B171-4	anklet	Fig. 3, 5	Haerinck & Overlaet 2004a, p. 64-65, pl. 63, 146
WK.A102-5	anklet		Haerinck & Overlaet 2004a, p. 64-65, pl. 42
WK.A1-4	bracelet		Haerinck & Overlaet 2004a, p. 65-66, pl. 5
WK.B185-3	fibula	Fig. 3	Haerinck & Overlaet 2004a, p. 73, fig. 34, pl. 66, 150
WK.A76-5	finger ring		Haerinck & Overlaet 2004a, p. 66-67, pl. 37
WK.B200-1	finger ring		Haerinck & Overlaet 2004a, p. 66-67, pl. 69
WK.A92-4	finger ring		Haerinck & Overlaet 2004a, p. 66-67, pl. 40
WK.A94-5	finger ring		Haerinck & Overlaet 2004a, p. 66-67, pl. 40, 148
WK.B155-2	pin	Fig. 3	Haerinck & Overlaet 2004a, p. 72, fig. 33, pl. 60
WK.B186-4	pin		Haerinck & Overlaet 2004a, p. 72, pl. 66, 150
WK.A43-6	pin		Haerinck & Overlaet 2004a, p. 72, pl. 21
WK.A22-3	pin	Fig. 8	Haerinck & Overlaet 2004a, p. 72, pl. 12
WK.A140-5	pin	Fig. 3	Haerinck & Overlaet 2004a, p. 72, fig. 33, pl. 55, 150
WK.A68-6	ring		Haerinck & Overlaet 2004a, p. 67-68, pl. 36, 148
WK.A150-8	ring		Haerinck & Overlaet 2004a, p. 57, pl. 57
WK.A56-4	ring		Haerinck & Overlaet 2004a, p. 67-68, pl. 33
WK.A49-5	ring		Haerinck & Overlaet 2004a, p. 67-68, pl. 31
WK.B199-3	ring		Haerinck & Overlaet 2004a, p. 67-68, pl. 69
WK.B196-5	vessel	Fig. 11	Haerinck & Overlaet 2004a, p. 57, 62, pl. 69
WK.B157-3	vessel		Haerinck & Overlaet 2004a, p. 57, 62, pl. 60, 133
WK.B167-2	vessel	Fig. 12	Haerinck & Overlaet 2004a, p. 57, 62, pl. 62
WK.B194-4	vessel		Haerinck & Overlaet 2004a, p. 57, 62, pl. 68
WK.B183-6	vessel		Haerinck & Overlaet 2004a, p. 57, 62, pl. 65
WK.B192-4	vessel		Haerinck & Overlaet 2004a, p. 57, 62, pl. 67
WK.B169-5	vessel		Haerinck & Overlaet 2004a, p. 57, 62, pl. 62
WK.B198-6	vessel		Haerinck & Overlaet 2004a, p. 57, 62, pl. 69
WK.A22-4	vessel		Haerinck & Overlaet 2004a, p. 57, 62, pl. 12
WK.A25-5	vessel	Fig. 4	Haerinck & Overlaet 2004a, p. 58, 61, fig. 20, pl. 13, 135
WK.A133-7	vessel	Fig. 4	Haerinck & Overlaet 2004a, p. 57, 62, fig. 20, pl. 53
WK.A103-6	vessel	Fig. 4	Haerinck & Overlaet 2004a, p. 57, 62, fig. 20, pl. 43, 135
WK.A107-5	vessel		Haerinck & Overlaet 2004a, p. 57, 62, pl. 44
WK.A123-6	vessel	Fig. 4, 10	Haerinck & Overlaet 2004a, p. 58, 62, fig. 20, pl. 50
WK.A46-5	vessel	Fig. 9	Haerinck & Overlaet 2004a, p. 58, 61, pl. 29
WK.A77-6	vessel		Haerinck & Overlaet 2004a, p. 57, 62, pl. 37
WK.B152-6	vessel		Haerinck & Overlaet 2004a, p. 57, 62, pl. 59
WK.B154-5	vessel		Haerinck & Overlaet 2004a, p. 57, 62, pl. 60, 133
WK.A68-7	vessel		Haerinck & Overlaet 2004a, p. 57, 61, pl. 36, 134
WK.A54-7	vessel		Haerinck & Overlaet 2004a, p. 57, 61, pl. 32
WK.A59-8	vessel	Fig. 4, 5	Haerinck & Overlaet 2004a, p. 58, 61, fig. 20, pl. 34, 136
WK.A10-6	vessel	Fig. 4	Haerinck & Overlaet 2004a, p. 61, fig. 20, pl. 8, 143
WK.B191-3	macehead	Fig. 3, 6, 7, 15	Haerinck & Overlaet 2004a, p. 50-51, fig. 17, pl. 67, 126
WK.A5-6	macehead	Fig. 3, 6, 7, 13	Haerinck & Overlaet 2004a, p. 50-51, fig. 17, pl. 6, 126
WK.B181-4	macehead	Fig. 3, 6, 7, 14	Haerinck & Overlaet 2004a, p. 50-51, fig. 17, pl. 64, 125
WK.A150-5	button	Fig. 3, 5, 7, 16	Haerinck & Overlaet 2004a, p. 55, 57, fig. 19, pl. 57, 128
WK.A150-9	button	Fig. 3, 7, 17	Haerinck & Overlaet 2004a, p. 55, 57, fig. 19, pl. 57, 128
WK.A150-12	bell	Fig. 3, 5, 7, 18	Haerinck & Overlaet 2004a, p. 55-57, fig. 19, pl. 57, 128



Fig. 2. View of the graveyard at War Kabud (1966). Note the pits of the illegal excavations around the rectangular excavated area of the Belgian Expedition.

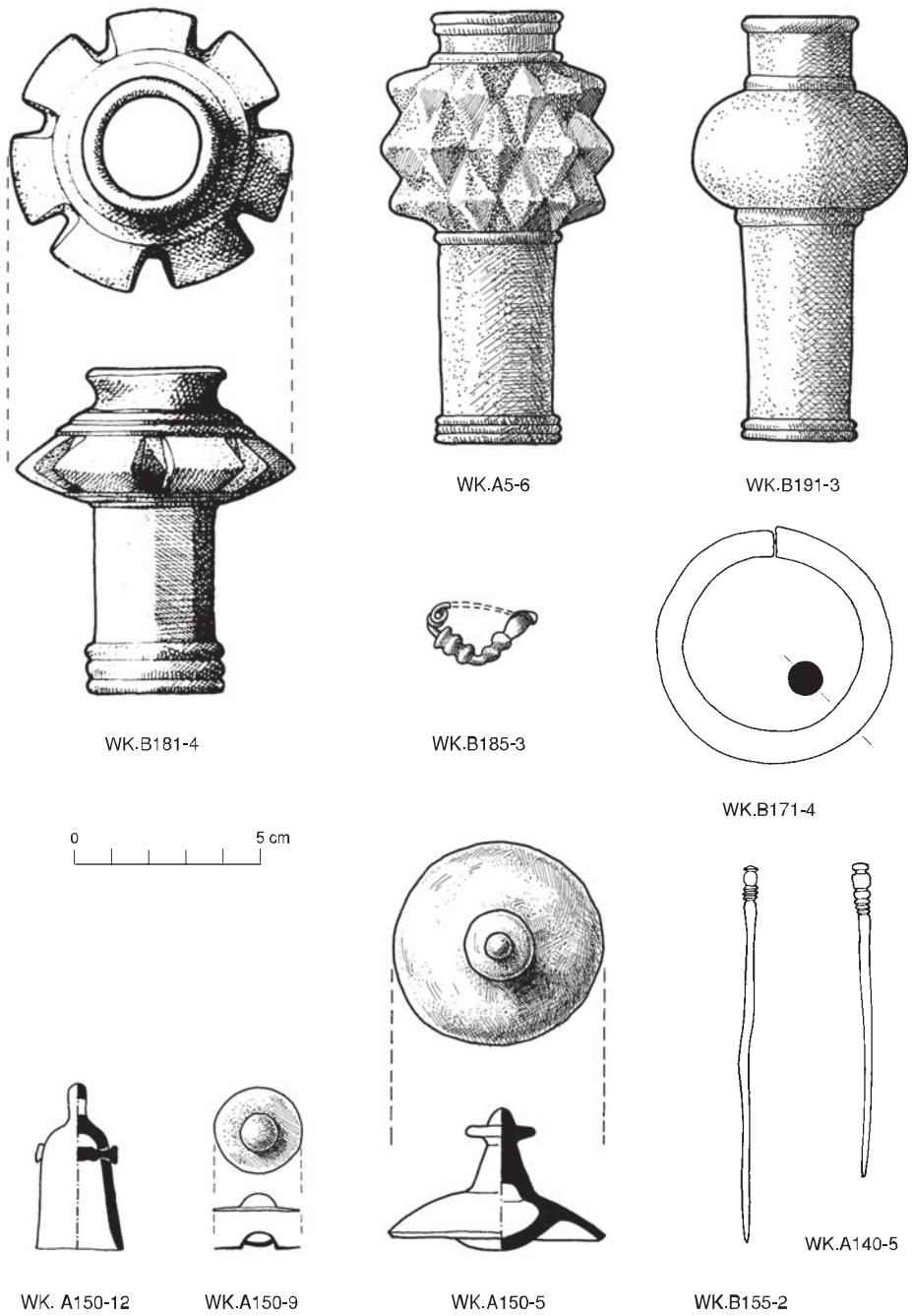
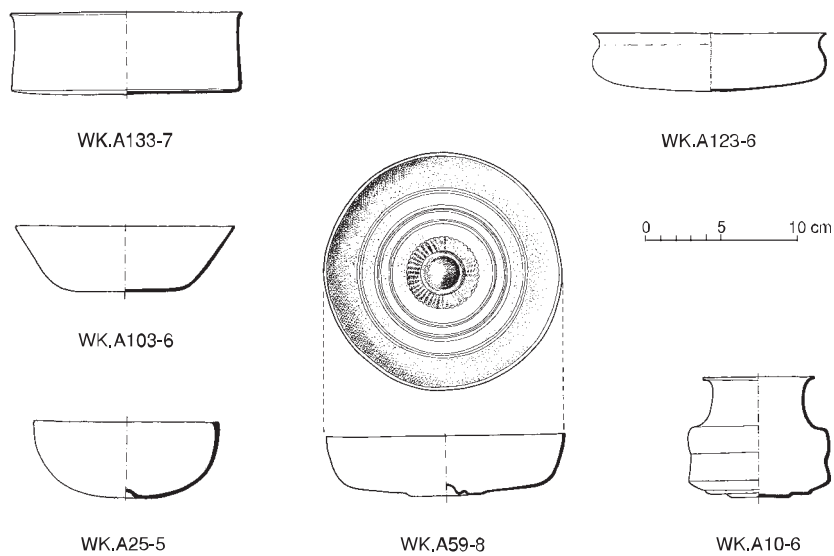


Fig. 3. Selection of the analysed bronze objects from War Kabud: maceheads, fibula, anklet, bell, buttons and pins (scale 1:2).



WK.A10-6

Fig. 4. Selection of the analysed bronze vessels from War Kabud (drawings scale 1:5).



WK.A59-8



WK.A150 12



WK.A171 6



WK.A150-2



WK.A150-5

Fig. 5. Selection of the analysed bronze objects from War Kabud: vessel, bell, anklet and button.



WK.B191-3



WK.A5-6



WK.B181-4

Fig. 6. The three analysed bronze maceheads from War Kabud.

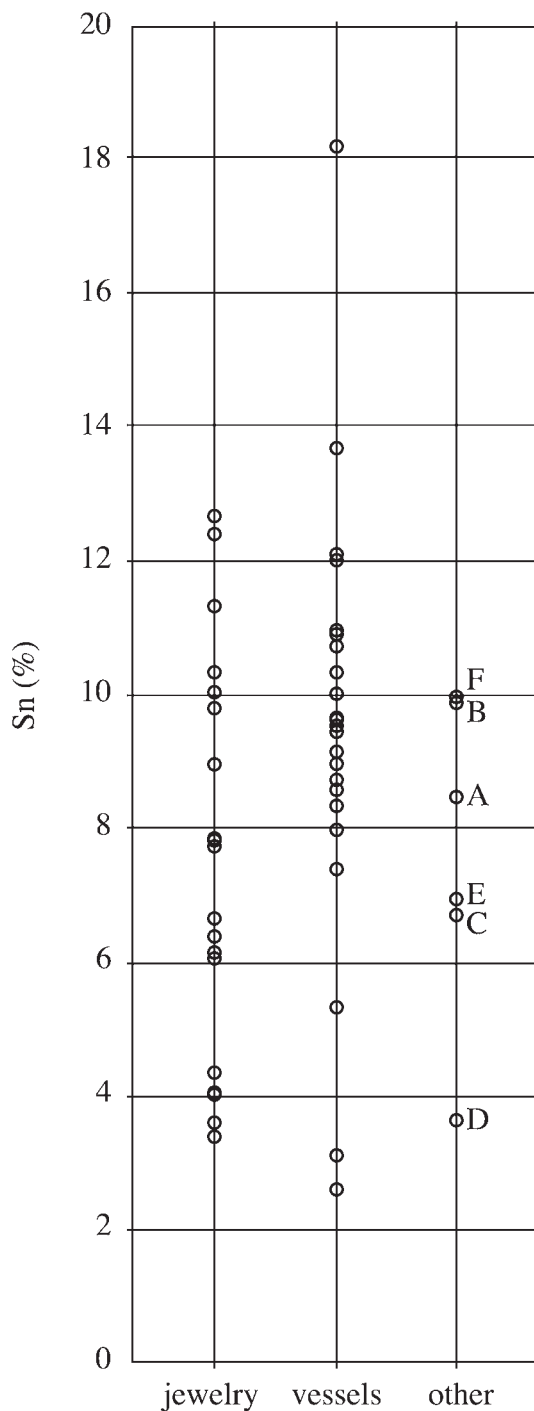


Fig. 7. A comparison of tin contents among War Kabud bronzes included in the MASCA analytical program, for jewellery, vessels, and the six other items. A: macehead (WK.B181-4); B: macehead (WK.A5-6); C: macehead (WK.B191-3); D: bell (WK.A150-12); E: button (WK.A150-5); F: button (WK.A150-9). — Graphic by Lindsay Shafer, MASCA.



Fig. 8. Micrograph for the pin (WK.A22-3) at a magnification of 100 \times , for a cross-section cut from midway down the shaft, where the tip is broken off. Etchant: potassium bichromate + alcoholic ferric chloride (Sn, 9.0%; As, 0.33%) The microstructure of this pin's circular cross-section displays a porous central area that most likely was formed by pockets of gas entrapped during casting, and a gross lap-seam that extends almost to the pin's center. Strain markings in the fine, re-crystallized grains of the metal, together with the flow pattern of numerous globular inclusions, indicates the direction in which the metal was shaped by a final cold-working.

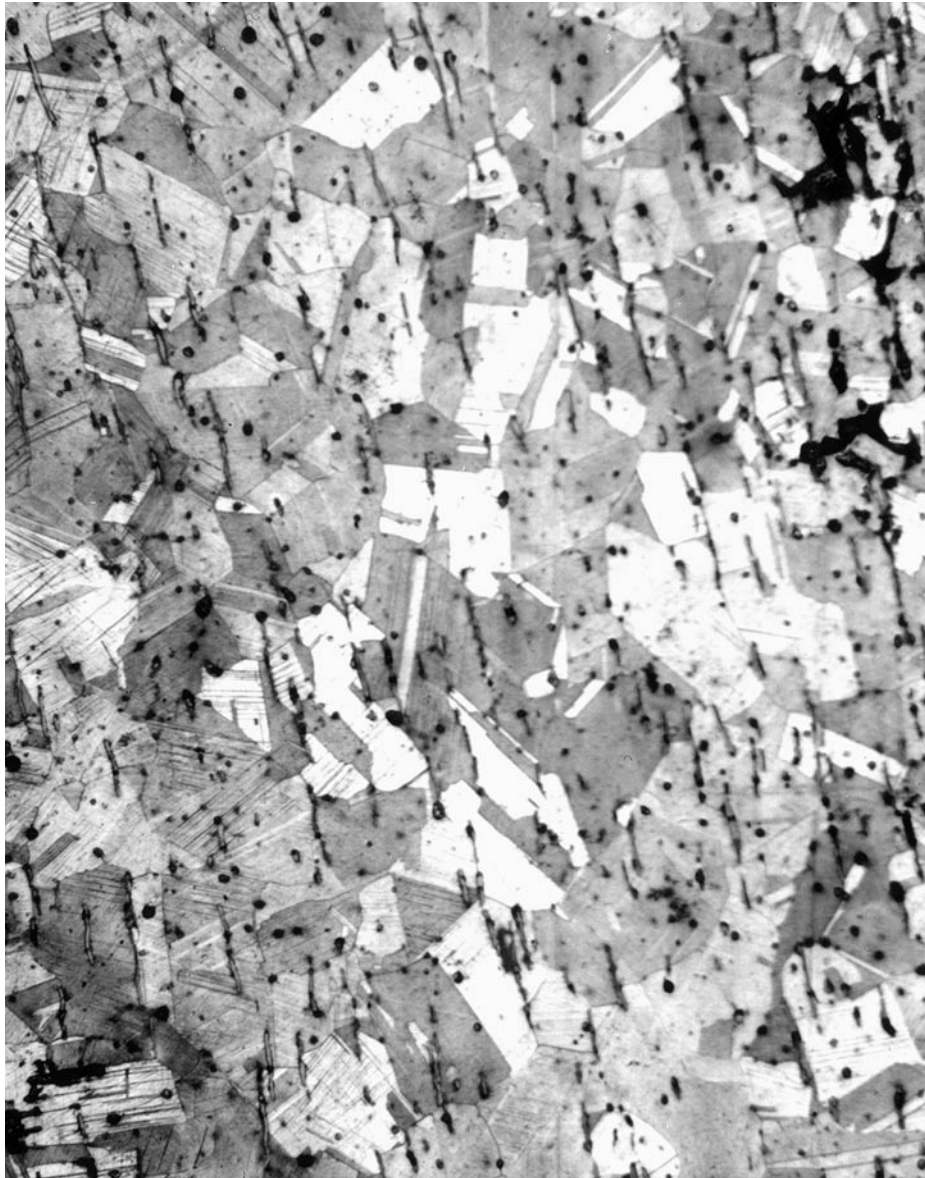


Fig. 9. Micrograph for the vessel (WK.A46-5) at a magnification of 200 \times ,
for a v-shaped section cut from the rim.

Etchant: potassium bichromate + alcoholic ferric chloride (Sn, 9.5%; As, 0.33%)

This microstructure, which displays appreciable variation in the grain size, indicates that the rim was hammered non-uniformly along its length prior to the final annealing treatment.

A high density of elongated inclusions closely follow the line of that rim as well.

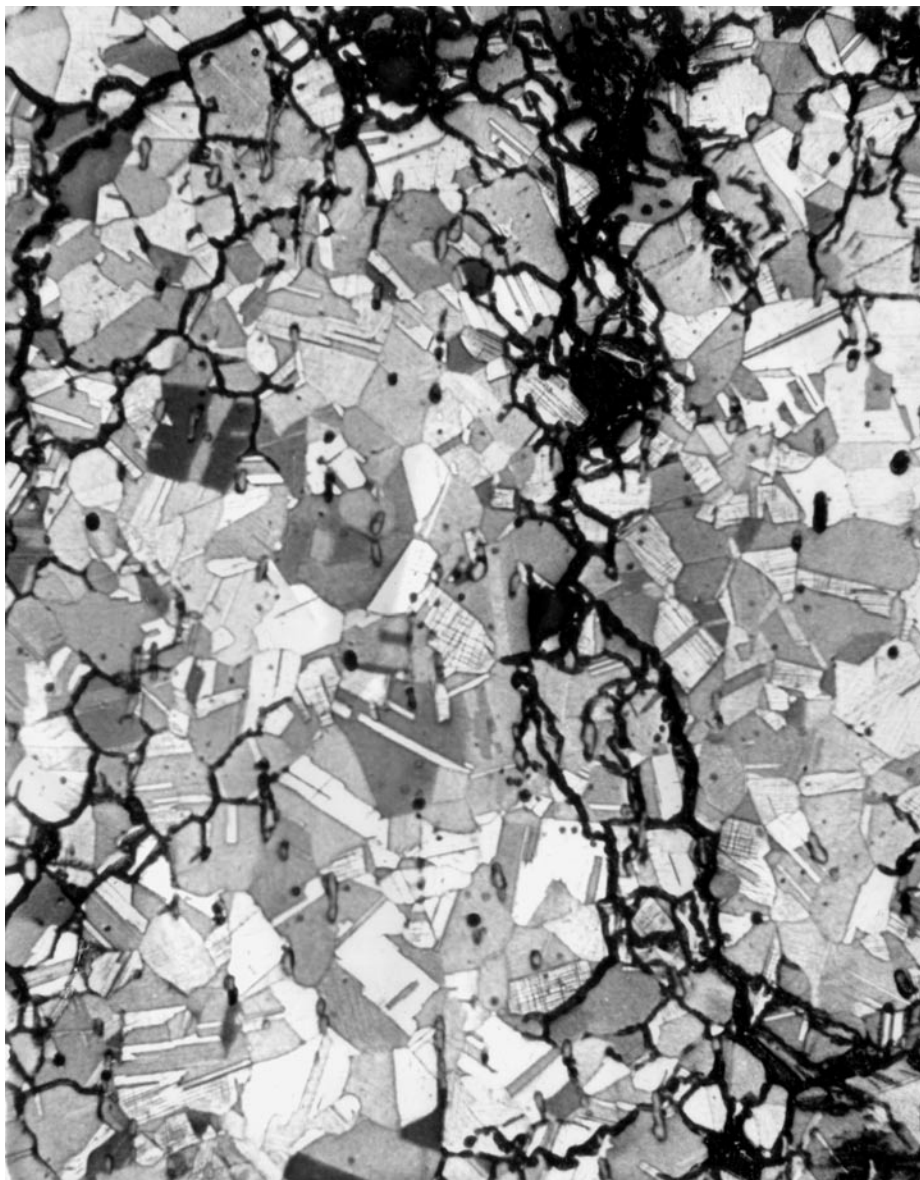


Fig. 10. Micrograph for the vessel (WK.A123-6) at a magnification of 200 \times , for a section cut off a fracture in the vessel's side wall, at the rim.

Etchant: Klemm's III (Sn, 18.2%; As, 0.06%)

The interior metal of this vessel is heavily penetrated by intergranular and pitting corrosion. But the remaining sound metal, with its high density of strain markings, tells us that the final treatment of the vessel's rim involved hot-working. As with WK.A46-5 (Figure 9 here), that working resulted in an alignment of inclusions along the rim's length.



Fig. 11. Micrograph for the vessel (WK.B196-5) at a magnification of 200 \times , for a v-shaped section cut from the rim.

Etchant: ammonium hydroxide + hydrogen peroxide (Sn, 3.1%; As, 0.51%)
This banded microstructure, with its fine grains that are re-crystallized, elongated and frequently twinned, indicates that the cup's rim was heavily deformed by both hot- and cold-working. That cold-working resulted in inclusions, which probably are sulfides, being elongated, aligned in the direction of working, and sometimes fractured.



Fig. 12. Micrograph for the vessel (WK.B167-2) at a magnification of 600 \times ,
for a v-shaped section cut from the rim.

Etchant: Klemm's III (Sn, 6.94%; As, 0.71%)

This microstructure, with its appreciable deformation and banding, reflects chemical segregation in the original alloy. In this instance, the cold-working of the vessel's rim was particularly heavy (cf., the treatment of other vessel rims described in figures 10 and 11), and the re-crystallization temperature was so low that the twinned grains are only visible at the high magnification of 600 \times used here.

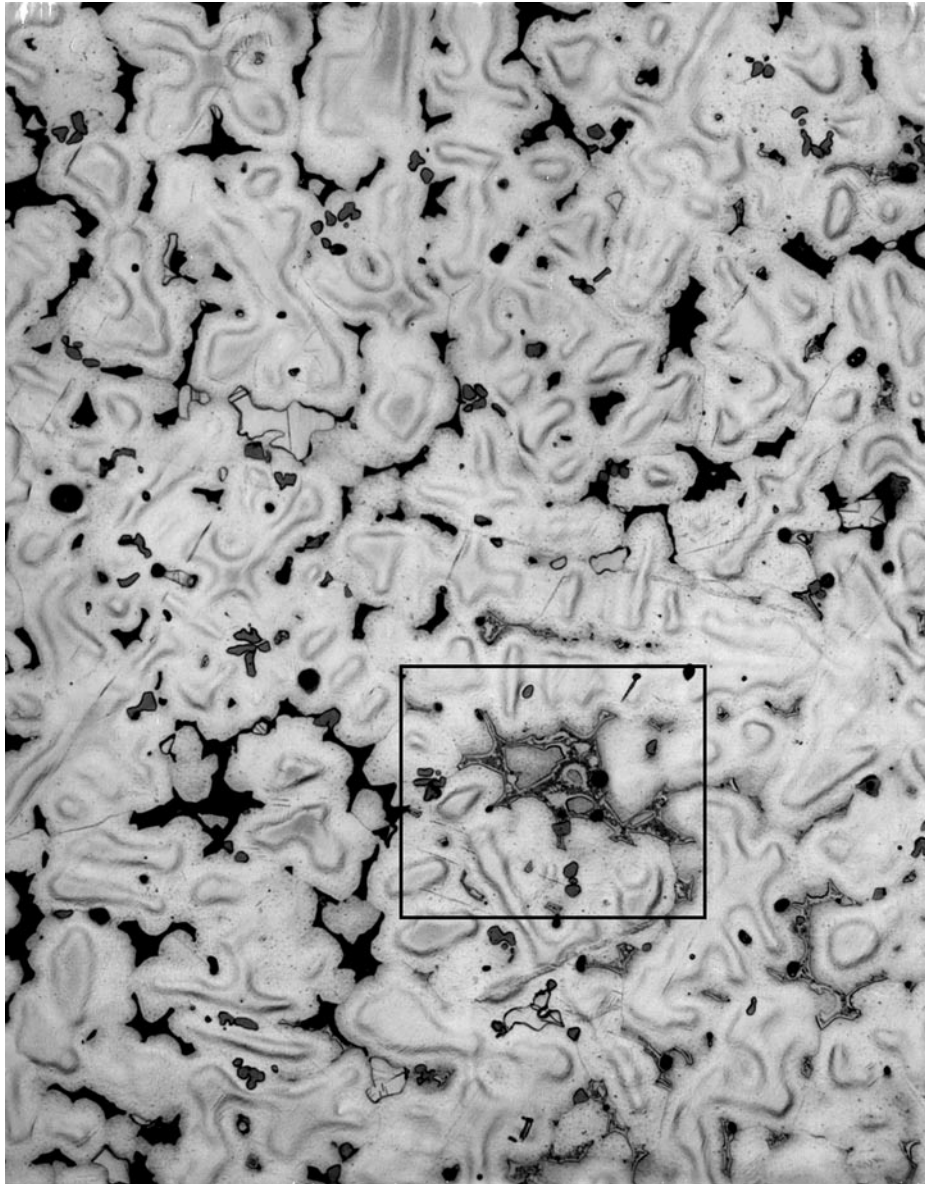


Fig. 13. Micrograph for the macehead (WK.A5-6) at a magnification of 200 \times , for a v-shaped section cut from the rim of the longer ferrule that is decorated with three circlets.

Etchant: potassium bichromate + alcoholic ferric chloride (Sn, 9.9%; As, 0.25%)

This microstructure, with its fully formed cored dendrites, extensive patches of interdendritic α - δ eutectoid, and appreciable interdendritic porosity, indicates that this artifact cooled quite rapidly during casting. Corrosion of some of the α - δ eutectoid has resulted in the formation of several islands of re-deposited copper (see boxed detail).



Fig. 14. Micrograph for the macehead (WK.B181-4) at a magnification of 200 \times , for a v-shaped section cut from the rim of the longer ferrule that is decorated with three circlets.
Etchant: potassium bichromate + alcoholic ferric chloride (Sn, 8.5%; As, 0.62%)
This microstructure, with its fully formed cored dendrites and a high density of interdentritic α - δ eutectoid, indicates that this artifact cooled quite rapidly during casting. The size of dendrites varies from place-to-place, though on the whole they are fairly coarse.

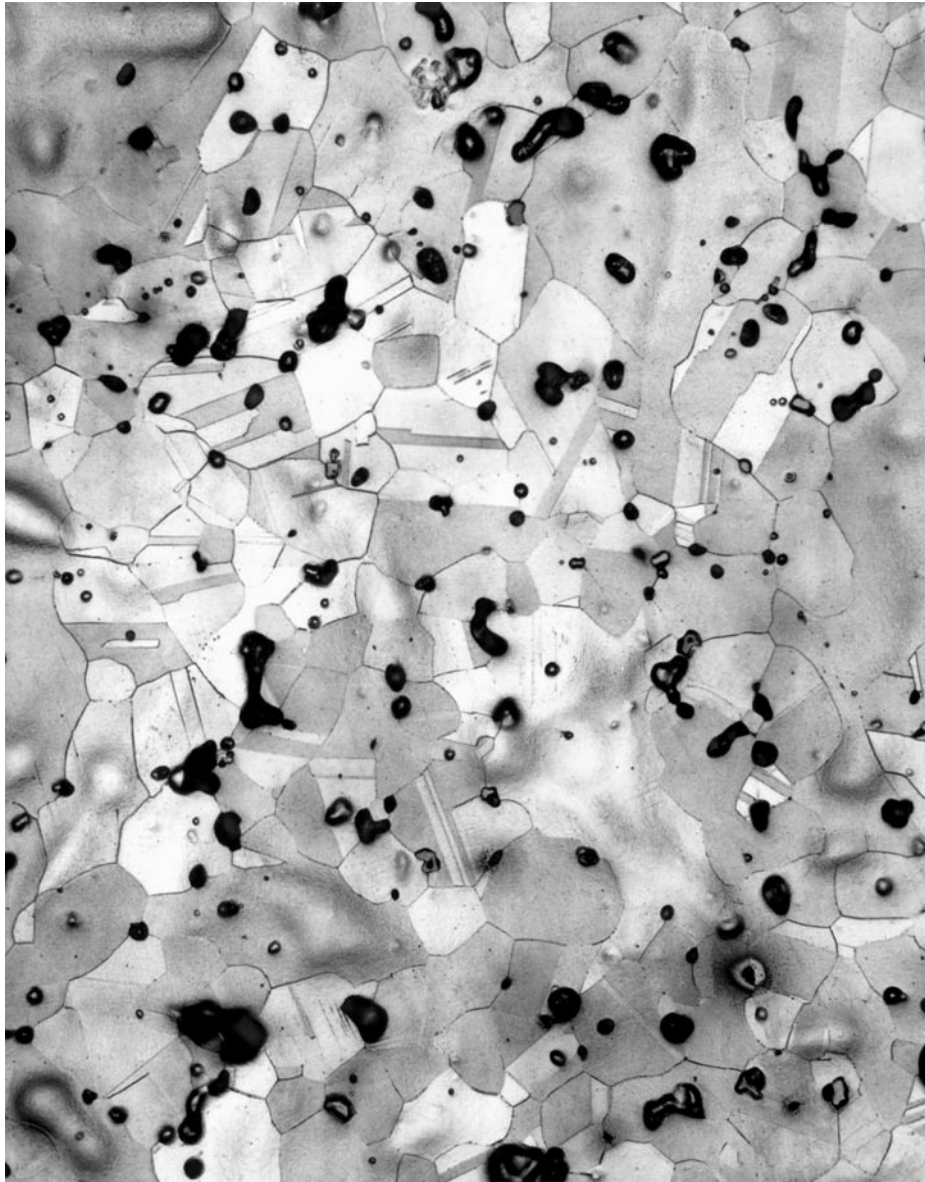


Fig. 15. Micrograph for the macehead (WK.B191-3) at a magnification of 200 \times , for a v-shaped section cut from the rim of the longer ferrule that is decorated with two circlets.

Etchant: potassium bichromate + alcoholic ferric chloride (Sn, 6.7%; As, 0.35%)

The microstructure, with its large twinned grains, indicates that the artifact was cast, then cold-worked and annealed, at least at its surface, perhaps to repair a casting irregularity (cf., the as-cast microstructures of the maceheads described in figures 13 and 14).

Deeper within the macehead's body, where the metal was much less effected by working, etching revealed a relief of cored dendrites. Considerable porosity and interdendritic shrinkage are evident throughout.

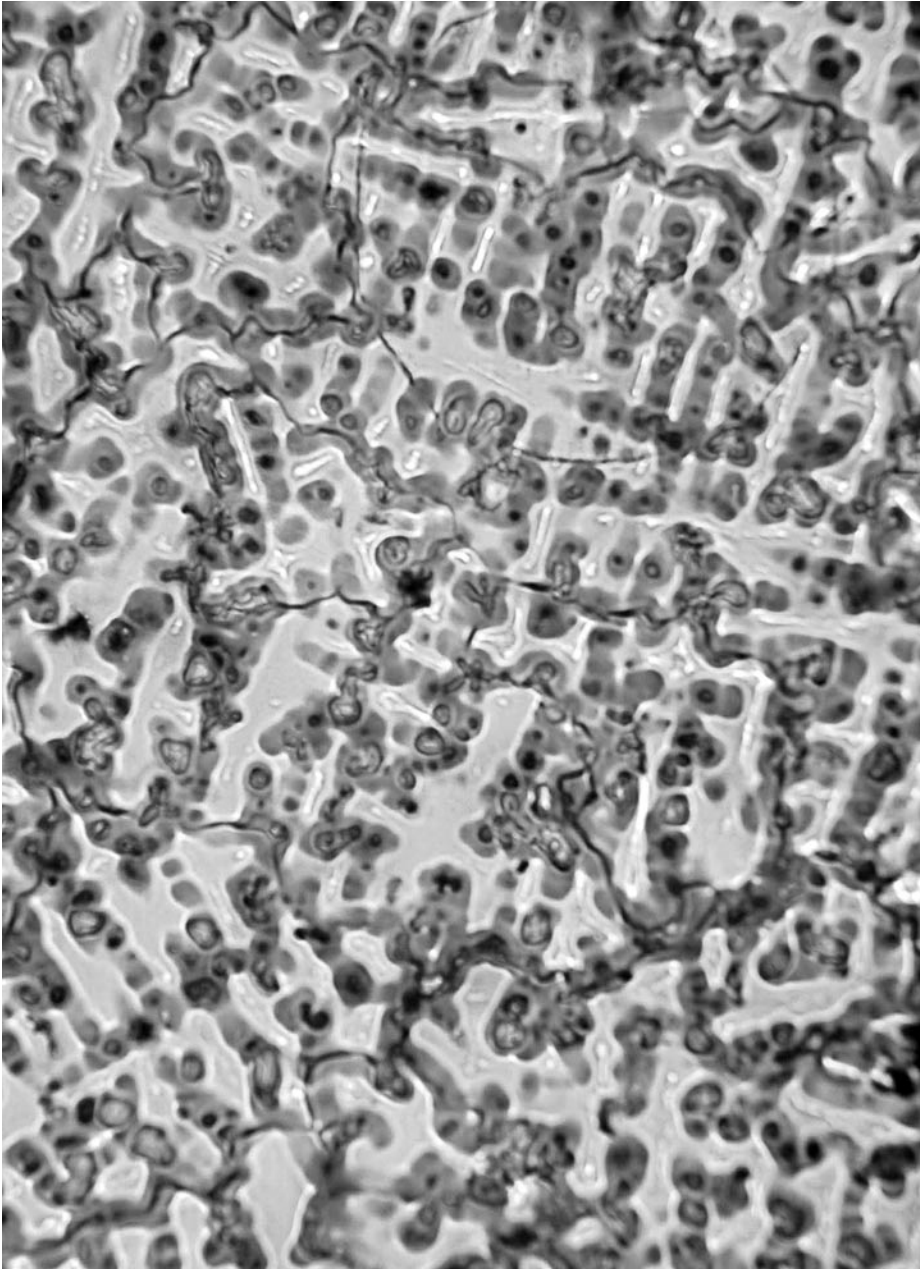


Fig. 16. Micrograph for the large button (WK.A150-5) at a magnification of 100 \times , for a v-shaped section cut from the edge.

Etchant: ammonium hydroxide + hydrogen peroxide + alcoholic ferric chloride
(Sn, 2.6%; As, 0.41%)

The microstructure has the array of cored dendrites that are characteristic of bronze casting. In addition to the typical interdendritic sulphide inclusions, α - δ eutectoid is present in these areas as well. The artifact must have gone through rapid solidification, perhaps because it is relatively thin, but not through a subsequent homogenizing heat treatment that would have dissolved the non-equilibrium α - δ eutectoid.



Fig. 17. Micrograph for the small button (WK.A150-9) at a magnification of 200 \times , for a v-shaped section cut from the rim.

Etchant: potassium bichromate + Klemm's III (Sn, 10.0%; As, =0.010%)

In this micrograph, the inherent segregation of tin in the alloy is manifested as banding superimposed upon polyhedral grains. This alloy must have been worked (i.e., deformed and annealed), as indicated by the lack of any α - δ eutectoid that may have been present at the time of casting. A final shaping operation, by hammering, is evident in the strain markings that are visible throughout the cross-section. This hammering was not sufficiently heavy, however, to cause the grains to be noticeably flattened or distorted.

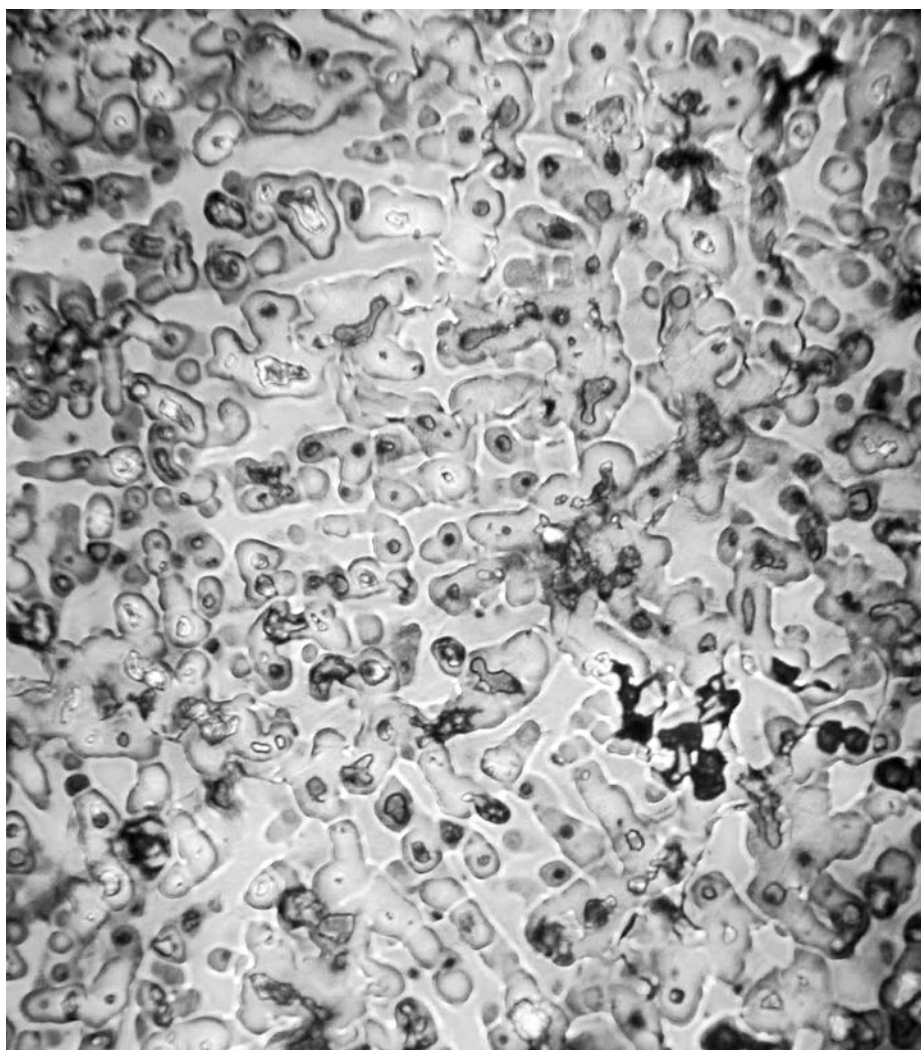


Fig. 18. Micrograph for the bell (inv. WK.A150-12: illustrated in plate 57,128) at a magnification of 200x, for a v-shaped section cut at the edge of the bell cavity.

Etchant: ammonium hydroxide + hydrogen peroxide + alcoholic ferric chloride
(Sn, 3.6%; As, 1.4%)

This microstructure displays all the typical earmarks of a casting—cored dendrites, a high density of sulphide-type inclusions, and, here and there, an island of α - δ eutectoid. Interdendritic shrinkage voids are present throughout. There was no post-casting annealing treatment.